

## Management of P in Agricultural Systems



- 1769 Diffuse pollution: A hidden threat to the water environment of the developing world  
Chengqing Yin, and Xiaoyan Wang
- 1770 Managing agricultural phosphorus for water quality: Lessons from the USA and China  
Andrew Sharpley, and Xiaoyan Wang
- 1783 Uncertainty analyses on the calculation of water environmental capacity by an innovative holistic method and its application to the Dongjiang River  
Qiuwen Chen, Qibin Wang, Zhijie Li, and Ruonan Li
- 1791 Settling basin design in a constructed wetland using TSS removal efficiency and hydraulic retention time  
Soyoung Lee, Marla C. Maniquiz-Redillas, and Lee-Hyung Kim
- 1797 Contribution of atmospheric nitrogen deposition to diffuse pollution in a typical hilly red soil catchment in southern China  
Jianlin Shen, Jieyun Liu, Yong Li, Yuyuan Li, Yi Wang, Xuejun Liu, and Jinshui Wu
- 1806 Determination of nitrogen reduction levels necessary to reach groundwater quality targets in Slovenia  
Miso Andelov, Ralf Kunkel, Jože Uhan, and Frank Wendland
- 1818 Integral stormwater management master plan and design in an ecological community  
Wu Che, Yang Zhao, Zheng Yang, Junqi Li, and Man Shi
- 1824 Investigation on the effectiveness of pretreatment in stormwater management technologies  
Marla C. Maniquiz-Redillas, Franz Kevin F. Geronimo, and Lee-Hyung Kim
- 1831 Assessment of nutrient distributions in Lake Champlain using satellite remote sensing  
Elizabeth M. Isenstein, and Mi-Hyun Park
- 1837 Acute toxicity evaluation for quinolone antibiotics and their chlorination disinfection processes  
Min Li, Dongbin Wei, and Yuguo Du
- 1843 Occurrence, polarity and bioavailability of dissolved organic matter in the Huangpu River, China  
Qianqian Dong, Penghui Li, Qinghui Huang, Ahmed A. Abdelhafez, and Ling Chen
- 1851 A comparative study of biopolymers and alum in the separation and recovery of pulp fibres from paper mill effluent by flocculation  
Sumona Mukherjee, Soumyadeep Mukhopadhyay, Agamuthu Pariatamby, Mohd. Ali Hashim, Jaya Narayan Sahu, and Bhaskar Sen Gupta
- 1861 Performance and microbial response during the fast reactivation of Anammox system by hydrodynamic stress control  
Yuan Li, Zhenxing Huang, Wenquan Ruan, Hongyan Ren, and Hengfeng Miao
- 1869 Phytoremediation of levonorgestrel in aquatic environment by hydrophytes  
Guo Li, Jun Zhai, Qiang He, Yue Zhi, Haiwen Xiao, and Jing Rong
- 1874 Experimental study on the impact of temperature on the dissipation process of supersaturated total dissolved gas  
Xia Shen, Shengyun Liu, Ran Li, and Yangming Ou
- 1879 Removal of cobalt(II) ion from aqueous solution by chitosan-montmorillonite  
Hailin Wang, Haoqing Tang, Zhaotie Liu, Xin Zhang, Zhengping Hao, and Zhongwen Liu
- 1885 *p*-Cresol mineralization and bacterial population dynamics in a nitrifying sequential batch reactor  
Carlos David Silva, Lizeth Beristain-Montiel, Flor de María Cuervo-López, and Anne-Claire Texier

## CONTENTS

- 1894 Particle number concentration, size distribution and chemical composition during haze and photochemical smog episodes in Shanghai  
Xuemei Wang, Jianmin Chen, Tiantao Cheng, Renyi Zhang, and Xinming Wang
- 1903 Properties of agricultural aerosol released during wheat harvest threshing, plowing and sowing  
Chiara Telloli, Antonella Malaguti, Mihaela Mircea, Renzo Tassinari, Carmela Vaccaro, and Massimo Berico
- 1913 Characteristics of nanoparticles emitted from burning of biomass fuels  
Mitsuhiko Hata, Jiraporn Chomanee, Thunyapat Thongyen, Linfa Bao, Surajit Tekasakul, Perapong Tekasakul, Yoshio Otani, and Masami Furuuchi
- 1921 Seasonal dynamics of water bloom-forming *Microcystis* morphospecies and the associated extracellular microcystin concentrations in large, shallow, eutrophic Dianchi Lake  
Yanlong Wu, Lin Li, Nanqin Gan, Lingling Zheng, Haiyan Ma, Kun Shan, Jin Liu, Bangding Xiao, and Lirong Song
- 1930 Mitochondrial electron transport chain is involved in microcystin-RR induced tobacco BY-2 cells apoptosis  
Wenmin Huang, Dunhai Li, and Yongding Liu
- 1936 Synthesis of novel CeO<sub>2</sub>-BiVO<sub>4</sub>/FAC composites with enhanced visible-light photocatalytic properties  
Jin Zhang, Bing Wang, Chuang Li, Hao Cui, Jianping Zhai, and Qin Li
- 1943 Investigation of UV-TiO<sub>2</sub> photocatalysis and its mechanism in *Bacillus subtilis* spore inactivation  
Yiqing Zhang, Lingling Zhou, and Yongji Zhang
- 1949 Rapid detection of multiple class pharmaceuticals in both municipal wastewater and sludge with ultra high performance liquid chromatography tandem mass spectrometry  
Xiangjuan Yuan, Zhimin Qiang, Weiwei Ben, Bing Zhu, and Junxin Liu

Available online at [www.sciencedirect.com](http://www.sciencedirect.com)

ScienceDirect

[www.journals.elsevier.com/journal-of-environmental-sciences](http://www.journals.elsevier.com/journal-of-environmental-sciences)

# Particle number concentration, size distribution and chemical composition during haze and photochemical smog episodes in Shanghai

Xuemei Wang<sup>1</sup>, Jianmin Chen<sup>1,\*</sup>, Tiantao Cheng<sup>1</sup>, Renyi Zhang<sup>2,\*</sup>, Xinming Wang<sup>3</sup>

1. Shanghai Key Laboratory of Atmospheric Particle Pollution and Prevention (LAP<sup>3</sup>), Fudan Tyndall Centre,

Department of Environmental Science & Engineering, Fudan University, Shanghai 200433, China. E-mail: [xuemeiwan@fudan.edu.cn](mailto:xuemeiwan@fudan.edu.cn)

2. Center for Atmospheric Chemistry and Environment, Department of Atmospheric Science, Texas A&M University, TX 77843, USA

3. State Key Laboratory of Organic Geochemistry, Guangzhou Institute of Geochemistry, Chinese Academy of Sciences, Guangzhou 510640, China

## ARTICLE INFO

### Article history:

Received 13 November 2013

Revised 23 December 2013

Accepted 10 January 2014

Available online 15 July 2014

### Keywords:

Haze

Photochemical smog

Particle number concentration

Size distribution

Chemical composition

Shanghai

## ABSTRACT

The aerosol number concentration and size distribution as well as size-resolved particle chemical composition were measured during haze and photochemical smog episodes in Shanghai in 2009. The number of haze days accounted for 43%, of which 30% was severe (visibility < 2 km) and moderate ( $2 \text{ km} \leq \text{visibility} < 3 \text{ km}$ ) haze, mainly distributed in winter and spring. The mean particle number concentration was about  $17,000/\text{cm}^3$  in haze, more than 2 times that in clean days. The greatest increase of particle number concentration was in  $0.5\text{--}1 \mu\text{m}$  and  $1\text{--}10 \mu\text{m}$  size fractions during haze events, about 17.78 times and 8.78 times those of clean days. The largest increase of particle number concentration was within  $50\text{--}100 \text{ nm}$  and  $100\text{--}200 \text{ nm}$  fractions during photochemical smog episodes, about 5.89 times and 4.29 times those of clean days. The particle volume concentration and surface concentration in haze, photochemical smog and clean days were  $102, 49, 15 \mu\text{m}^3/\text{cm}^3$  and  $949, 649, 206 \mu\text{m}^2/\text{cm}^3$ , respectively. As haze events got more severe, the number concentration of particles smaller than  $50 \text{ nm}$  decreased, but the particles of  $50\text{--}200 \text{ nm}$  and  $0.5\text{--}1 \mu\text{m}$  increased. The diurnal variation of particle number concentration showed a bimodal pattern in haze days. All soluble ions were increased during haze events, of which  $\text{NH}_4^+$ ,  $\text{SO}_4^{2-}$  and  $\text{NO}_3^-$  increased greatly, followed by  $\text{Na}^+$ ,  $\text{K}^+$ ,  $\text{Ca}^{2+}$  and  $\text{Cl}^-$ . These ions were very different in size-resolved particles during haze and photochemical smog episodes.

© 2014 The Research Center for Eco-Environmental Sciences, Chinese Academy of Sciences.

Published by Elsevier B.V.

## Introduction

High concentrations of particles can affect light absorption and scattering, thus impacting regional visibility and climate. They can also degrade air quality and pose a threat to human health. In

recent years, haze events caused by fine particle pollution in megacities have occurred more and more frequently. Impaired visibility has become a hot topic in atmospheric research. In 2010, the industry standard for the observation and forecasting levels of haze (QX/T 113-2010) was promulgated and implemented by

\* Corresponding authors. E-mail: [jmchen@fudan.edu.cn](mailto:jmchen@fudan.edu.cn) (Jianmin Chen), [renyi-zhang@neo.tamu.edu](mailto:renyi-zhang@neo.tamu.edu) (Renyi Zhang).



the China Meteorological Administration. In 2012, the new air quality standard was put in place in China, in which the standard for PM<sub>2.5</sub> daily average concentration was set at 75 µg/m<sup>3</sup>. In addition, regulatory monitoring networks for PM<sub>2.5</sub> were built in different cities across the country (Yuan et al., 2012).

So far, most haze studies in China have been in the North China Plain, in which Beijing is located (Tao et al., 2012; T. Yang et al., 2012; Li et al., 2009, 2010, 2011; Guo et al., 2012a; Duan et al., 2012; Ma et al., 2010; Wang et al., 2006; Z.T. Wang et al., 2012; Sun et al., 2006; Yu et al., 2011), and the Pearl River Delta region, where Guangzhou is situated (Wu et al., 2007; Tan et al., 2009, 2011; Chen et al., 2009; Guo et al., 2012b; X.M. Wang et al., 2012; Lu et al., 2009; Andreae et al., 2008; Xu et al., 2008). Most of these studies involve particle mass concentration, composition and optical properties in haze, while very few studies (Quan et al., 2011; Chen et al., 2012a) have looked at the particle number concentration and size distribution. In the study by Quan et al. (2011), the number concentration of dry aerosols (relative humidity (RH) < 40%) in the size range of 10–662 nm was as high as 24,000/cm<sup>3</sup> during the period of dense haze mixed with fog on the North China Plain from November 5th to 8th, 2009. The formation of fog was increased with the large amount of particles serving as nuclei, leading to extremely low visibility of less than 100 m. Chen et al. (2012a,b) found that the average number concentration and volume concentration of dry particles (RH < 30%) in the size range of 3 nm–10 µm were 17,200/cm<sup>3</sup> and 70.9 µm<sup>3</sup>/cm<sup>3</sup>, respectively, during another haze event on the North China Plain from July 13th to August 14th, 2009. They found that when RH < 90%, high particle volume concentration contributed more to visibility impairment than the increase of RH. However, they did not measure the size distribution. Although Shanghai is the largest megacity in the Yangtze River Delta region (YRD), there have been a few studies on haze here (Fu et al., 2008; Chen et al., 2012b; F. Yang et al., 2012; Huang et al., 2012; Du et al., 2011; Ye et al., 2011; Hou et al., 2011), mainly on chemical composition. Few results have been reported on particle number concentration, chemical composition and size distribution in haze in Shanghai, and studies focused on both haze and air oxidation have been rare.

However, photochemical smog, characterized by high ozone and other oxidant levels, has remained one of the severe environmental problems of the YRD (Ma et al., 2012). Frequent adverse effects of elevated ozone levels on the air quality were becoming a cause for concern from early summer to early autumn, even though no haze events appeared. Ozone pollution contributed to heart and respiratory disease, especially to susceptible groups (Zhang et al., 2006). Most days of high ozone concentration could easily be overlooked by the public when no haze was present.

To obtain a more complete picture on the characterization of haze and photochemical smog in this coastal megacity as well as the processes of their formation and removal, additional data were needed. In this study, we reported the occurrence frequency of different levels of haze and ozone concentration during the year, and measured the aerosol number concentration, size distribution and size-resolved particle chemical compositions at Fudan University, an urban site in Shanghai, during haze and photochemical smog episodes in 2009. The conclusions and suggestions

provide reference data for decision making by air pollution treatment administrators.

## 1. Material and methods

### 1.1. Description of sampling sites

Sampling sites were located at the roof of a five-story building, about 20 m above ground, in the campus of Fudan University. The campus is in a commercial and residential area. The sampling inlet was set up according to standard air quality monitoring methods.

### 1.2. Sampling instruments and sample analysis

The Wide-Range Particle Spectrum 1000XP (MSP Company, Minneapolis, MN, USA) was used in this study. It could measure the number concentration of particles in size ranges from 10 nm to 10 µm, and the particle volume concentration and surface concentration could also be derived via predetermined algorithms. The instrument uses a Differential Mobility Analyzer (DMA) and Condensation Particle Counter (CPC) to measure particles between 10 nm and 0.5 µm and a Laser Particle Spectrometer (LPS) to measure particles between 0.35 and 10 µm. The instrument was calibrated with standard particle samples before and after sampling periods. It took about 3 min for one complete scan of the entire size range. More details on the instrument have been described elsewhere (Gao et al., 2009; Zhang et al., 2010).

Ozone was measured using a UV Photometric Ozone analyzer (Model 49i, Thermo Fisher Scientific Inc., Waltham, MA, USA), and was recorded each minute. Quality control checks were performed as per specifications including zero, precision and span checks. Filters were replaced every week, and calibration was carried out every three months.

An Andersen 1 ACFM Eight-stage Cascade Impactor (Thermo Fisher Scientific Inc., Waltham, MA, USA) was used for particle size-segregated sampling. The particle size ranges captured by the eight stages were 0.4–0.7, 0.7–1.1, 1.1–2.1, 2.1–3.3, 3.3–4.7, 4.7–5.8, 5.8–9.0 and 9.0–10 µm, respectively. Particles were collected with Whatman 41 fiber filters (GE Healthcare UK Ltd, Buckinghamshire, England), with a pore size of 0.2 µm. Filters were placed in a chamber with constant humidity (40 ± 1)% and temperature (20 ± 1)°C for 24 hr and then weighed with an electronic balance (accuracy = 10 µg), before and after sampling. Sampled filters were folded and wrapped with sulfuric acid paper and stored in sealed plastic bags refrigerated at –20°C for further analysis of chemical composition. Each sample and control was cut diagonally into 8 pieces before analysis. Two pieces were used to extract ions by ultrasound in 10 mL pure water (18 MΩ/cm<sup>3</sup>) for 20 min. The liquid was filtered with a microporous membrane and analyzed by ion chromatography. Ions measured in the analysis included Na<sup>+</sup>, NH<sub>4</sub><sup>+</sup>, K<sup>+</sup>, Mg<sup>2+</sup>, Ca<sup>2+</sup>, SO<sub>4</sub><sup>2-</sup>, NO<sub>3</sub><sup>-</sup>, Cl<sup>-</sup>, HCOOH<sup>-</sup>, C<sub>2</sub>H<sub>2</sub>OOH<sup>-</sup>, HNO<sub>2</sub><sup>-</sup> and F<sup>-</sup>.

### 1.3. Meteorological data

Meteorological parameters such as half-hour average visibility, RH and precipitation in 2009 were collected from [www.wunderground.com](http://www.wunderground.com).

## 2. Statistical analysis of haze events and ozone concentration

Using relevant meteorological data collected in 2009 in Shanghai, haze events could be categorized into severe haze (visibility < 2 km), moderate haze (2 km ≤ visibility < 3 km), light haze (3 km ≤ visibility < 5 km) and mild haze (5 km ≤ visibility < 10 km), according to the 2010 industry standard for haze. Impairment of visual range by weather events such as precipitation, fog and thunderstorm was excluded from the analysis. The results of the frequency of haze events in different categories in 2009 in Shanghai are presented in Fig. 1a.

Haze events occurred in a total of 156 days in Shanghai in 2009 and a third of these events were severe or moderate. They occurred mainly in winter and spring. The annual number of events was comparable to that observed in Hangzhou, where haze events occurred in about 160 days (Xiao et al., 2011), with similar seasonality. This further suggests that haze events in the YRD are usually regional events and relatively severe. The massive burning of agricultural residuals in and around Shanghai in June and October also led to reduced visibility and severe haze events during this period.

The hourly average ozone concentrations of the urban air in Shanghai in 2009 are shown in Fig. 1b as percentage frequencies. It was found that 0.65% of the hourly O<sub>3</sub> concentrations exceeded 160 ppbv, and 2.17% of the hourly contents exceeded 100 ppbv. Compared with the results in 2005 (Zhang et al., 2007), the non-attainment rate of O<sub>3</sub> concentration rose in Shanghai in 2009.

Through study of the correspondence between the actual date of haze events and the specific periods of high O<sub>3</sub> concentration, it was found that the lowest incidence of haze events was recorded in July, August and September, and that the months in which the hourly average O<sub>3</sub> concentration was over 100 ppbv were mostly in May, June, July and August (Table 1). June had the highest number of haze days among the 4 months with the highest O<sub>3</sub> concentration, followed by May. In May and June, the number of haze days in which the visibility was less than 10 km reached 50% of the total days of high O<sub>3</sub> concentration, and the other 50% was non-haze days. In July and August, the number of the haze days accounted for 30% and 20% of the total days of high O<sub>3</sub> concentration, and the other 70% and 80% were non-haze days, respectively. As a

result, such days with heavy O<sub>3</sub> pollution but without haze could easily be overlooked by the public. However, the proportion of such days was very high, and deserves attention.

## 3. Results and discussion

### 3.1. Particle number concentration and size distribution during haze and photochemical smog

The sampling period of particle number concentration and size distribution was from April 5th to June 8th, and all of the selected haze episodes lasted for more than 3 days in our research. All of the selected photochemical smog episodes also lasted for more than 3 days, in which the maximum of hourly average O<sub>3</sub> concentration exceeded 100 ppbv and haze was not present. The average visual ranges for haze, photochemical smog and clean days were 3 km, about 15 km and above 20 km, respectively. The RH was 66%, 56% and 58%, with average wind speeds of 1, 4 and 6 m/sec. In all three types of days, the number concentration of PM<sub>1</sub> accounted for more than 99.9% of the PM<sub>10</sub> number concentration (Table 2), suggesting that the major pollutant in Shanghai was ultrafine particles.

In clean days, the total particle number concentration was below 8000 /cm<sup>3</sup>, with 21.5% in nucleation mode (10–20 nm), 65.8% in Aitken mode (20–100 nm) and 12.6% in accumulation mode (100 nm–1 μm). Compared with 49,100 /cm<sup>3</sup> measured in clean days in Beijing (Shi et al., 2007), the total number concentrations were much lower. Possible explanations are that the clean days in Beijing were chosen in winter when coal was burned for heating, and the size ranges of the monitoring instrument were much wider than those in our study.

In haze days, the total particle number concentration was 17,000 /cm<sup>3</sup>, about 2.2 times that of clean days. This result was comparable to that observed in the North China Plain in 2009 by Chen et al. (2012a), with much lower concentration of particles in accumulation mode (3836 /cm<sup>3</sup> vs. 5320 /cm<sup>3</sup>), accounting for 22.8% and 30.9% of the total number concentrations, respectively.

During photochemical smog episodes, the total particle number concentration was 23,000 /cm<sup>3</sup>, about 3.2 times that of clean days and higher than that in haze days, with 11.0% in nucleation mode, 75.1% in Aitken mode and 13.8% in accumulation mode.

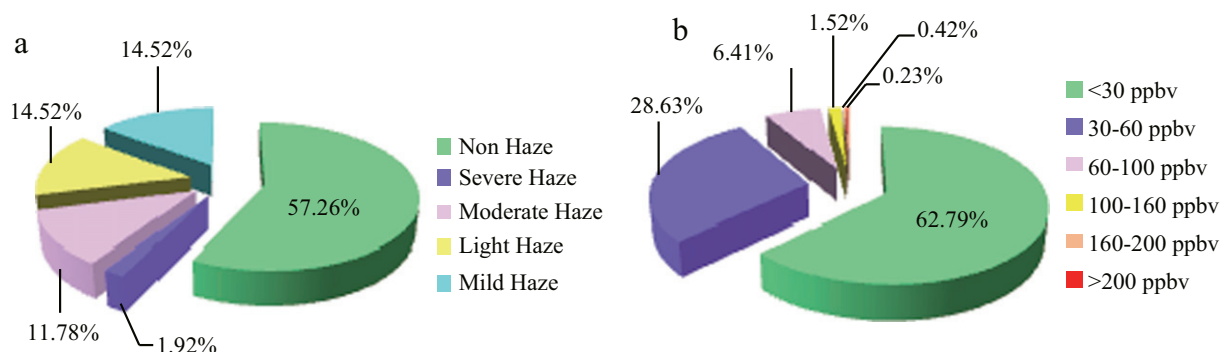


Fig. 1 – Frequency of haze events (a) and the hourly average of ozone concentration (b) in 2009, Shanghai.

**Table 1 – Frequency of the visibility and the hourly average of ozone concentration from January to December in 2009, Shanghai (%).**

Month	Visibility (km)					O <sub>3</sub> (ppbV)					
	<2	2–3	3–5	5–10	≥10	<30	30–60	60–100	100–160	160–200	≥200
January	0	16.1	16.1	22.6	45.2	92.7	7.3	0	0	0	0
February	0	17.9	7.1	7.1	67.9	76.3	22.2	1.5	0	0	0
March	3.2	16.1	12.9	16.1	51.6	56.7	40.8	2.6	0	0	0
April	0	13.3	20.0	16.7	50.0	36.7	43.8	19.1	0.5	0	0
May	0	6.5	12.9	16.1	64.5	28.2	49.9	18.7	3.2	0	0
June	6.7	13.3	13.3	10.0	56.7	38.2	31.4	11.9	10.9	4.9	2.7
July	0	3.2	9.7	9.7	77.4	61.3	25.5	11.3	1.9	0	0
August	0	6.5	3.2	3.2	87.1	65.4	28.0	5.4	1.2	0	0
September	0	0	13.3	20.0	66.7	61.8	36.4	1.8	0	0	0
October	0	19.4	25.8	22.6	32.3	49.5	46.2	4.2	0.1	0	0
November	6.7	10.0	16.7	13.3	53.3	90.5	8.9	0.6	0	0	0
December	6.5	19.4	22.6	16.1	35.5	99.1	0.9	0	0	0	0

In the three instances, particles in Aitken mode were predominant. However, comparing the proportions of particle modes in different types of days, the proportion of particles in accumulation mode was highest for haze days, and in Aitken mode for photochemical smog, while it was highest in nucleation mode for clean days. This suggests that the new formation of particles was limited in haze days while the accumulation and growth of particles was enhanced.

The particle number concentration ratios of haze to clean days and photochemical smog to clean days suggest that the particle number concentration increased to different extents in different size ranges. Particles larger than 200 nm increased more in haze days, while particles smaller than 100 nm increased during photochemical smog. The increase of particle number from 100 to 200 nm was almost the same for haze and photochemical smog. The greatest increase of particle number concentration in haze events occurred in the size ranges of 0.5–1 and 1–10  $\mu\text{m}$ , respectively 17.78 times and 8.78 times the values for clean days, while the largest increase from particle numbers within the ranges of 50–100 and 100–200 nm for photochemical smog were respectively 5.89 times and 4.29 times the clean days. This suggests that in haze days more particles were in large size ranges, exerting a great impact on visibility; while in photochemical smog, the increase of large particles was not apparent.

Fig. 2 presents the results of size distribution analysis. The particle size distribution had a larger range during haze events, with a tail extending up to 0.8  $\mu\text{m}$ , while the range for photochemical smog was narrower, mostly below 100 nm. The peak for clean days appeared around 30 nm and was the smallest. In addition, the results show that in haze days the

concentration of particles smaller than 150 nm was lower than that in photochemical smog, but the concentration of particles larger than 150 nm were higher.

The particle volume concentrations of haze, photochemical smog and clean days were 102, 49 and 15  $\mu\text{m}^3/\text{cm}^3$ , respectively. It was clearly found that the particle volume concentration for photochemical smog with the highest number concentration was only 48% of that of haze days. The concentration observed in haze events was 1.4 times the result (70.9  $\mu\text{m}^3/\text{cm}^3$ ) of Chen et al. (2012a) in the North China Plain. The higher total number concentration in accumulation mode in the North China Plain did not result in a higher volume concentration than in Shanghai, possibly due to the presence of more particles in smaller size ranges. But Chen et al. (2012a) did not further illustrate particles between 100 nm and 1  $\mu\text{m}$ , so the difference could also be due to differences in humidity conditions where the number concentration was measured. The results of our study suggest that particles larger than 200 nm only made up 5% of the number concentration under all conditions but around 90% of the total volume concentration, and particles larger than 1  $\mu\text{m}$  contributed 50% of the total volume concentration. The concentration of particles in this size range increased in haze days, and it was this increase that led to haze events. Generally speaking, the density of particles in different size ranges varies. The density of secondary particles in small size ranges is usually lower than that of coarse particles. As a result, we did not use a uniform density to calculate particle mass concentration.

The particle surface concentrations of haze, photochemical smog and clean days were 949, 649 and 206  $\mu\text{m}^2/\text{cm}^3$ ,

**Table 2 – Average number concentration of particles in different size fractions in haze, photochemical smog and clean days (unit:  $/\text{cm}^3$ ).**

Size	Haze	Clean	Photochemical smog	Haze/clean	Photochemical smog/clean
10–20 nm	1665	1622	2642	1.03	1.63
20–50 nm	6591	3580	9791	1.84	2.73
50–100 nm	4702	1389	8178	3.39	5.89
100–200 nm	2678	631	2704	4.25	4.29
200–500 nm	1030	317	579	3.25	1.82
0.5–1 $\mu\text{m}$	114	6	20	17.78	3.19
1–10 $\mu\text{m}$	14	2	5	8.78	3.23
10 nm–10 $\mu\text{m}$	16797	7547	23920	2.23	3.17

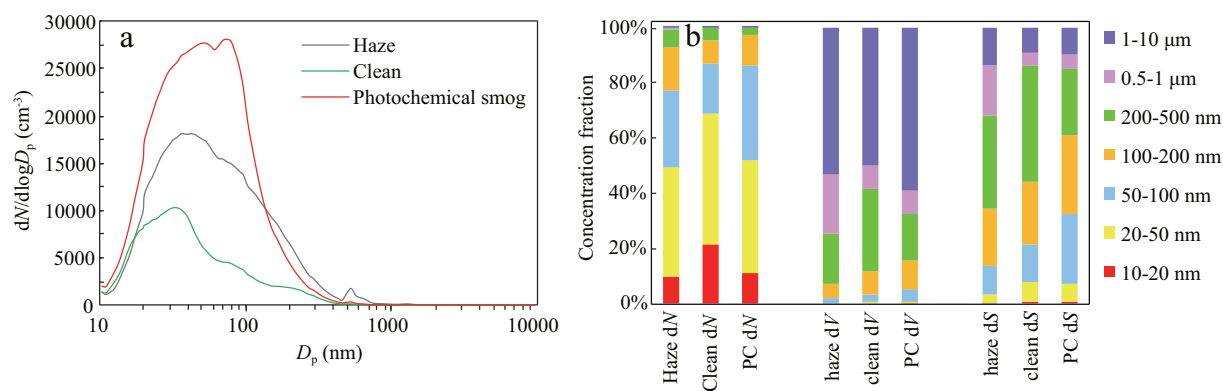


**Fig. 2 – Particle number size distribution ( $D_p$ ) (a) and average percentages of particle number (N), volume (V) and surface concentrations (S) in different size ranges (b) in haze, photochemical smog (PC) and clean days.**

respectively. The increase of surface concentration was smaller than volume concentration in haze days but larger in photochemical smog. This suggests that the large surface concentration favored the growth of small particles. Particles larger than 100 nm contributed about 90% of the surface concentration in haze days while only about 70% in photochemical smog, even less than in clean days. This suggests significant formation and growth of small particles during photochemical smog episodes.

### 3.2. Particle number concentration and size distribution during different levels of haze

As shown in Table 3, total particle number concentrations in severe, moderate and light hazes were higher than that in mild haze, but the concentration in severe haze was not the highest. As the severity of haze increased, the number concentration of particles smaller than 50 nm decreased while the concentrations of particles in the size ranges of 50–100 nm, 100–200 nm and 0.5–1 μm increased in order. The concentrations of particles in 10–20 nm declined greatly in severe haze, only 30% of that in moderate haze, and this can explain why the total number concentration was smaller in severe haze than in moderate and light haze. As shown in Fig. 3b, when the severity increased, the percentage of particles smaller than 50 nm decreased and particles larger than 50 nm increased. This suggests that the severity of haze was not simply determined by the increase of particle number concentration, but also closely related to the size distribution.

**Table 3 – Particle number concentration of different levels of haze (unit: /cm<sup>3</sup>).**

Size	Severe haze	Moderate haze	Light haze	Mild haze
10–20 nm	459	1590	1875	1816
20–50 nm	5486	6908	7185	6127
50–100 nm	6037	5297	4593	3378
100–200 nm	2829	2741	2324	1772
200–500 nm	886	974	895	762
0.5–1 μm	175	127	115	89
1–10 μm	12	14	14	10
10 nm–10 μm	15883	17652	17001	13954

As shown in Fig. 3a, the size distribution of particle number concentration in light and moderate haze was very similar, while the peak in severe haze shifted to larger size. As haze became more severe, particles in the large size range increased. This suggests that the increase of large particles was the determinant for haze severity.

Particle volume concentrations in severe, moderate, light and mild haze were 103, 102, 98 and 71 μm<sup>3</sup>/cm<sup>3</sup>, respectively. When the particle volume concentration was larger than 98 μm<sup>3</sup>/cm<sup>3</sup>, visibility was less than 5 km. Analysis by Chen et al. (2012a) suggested that when particle volume concentration was larger than 75 μm<sup>3</sup>/cm<sup>3</sup> in the North China Plain, visibility was less than 5 km. Notably, the percentage of particles in the size range of 0.5–1 μm was much higher in severe haze than in other three hazes.

The surface concentrations in severe, moderate, light and mild haze days were 1031, 969, 883 and 680 μm<sup>2</sup>/cm<sup>3</sup>, similar to the trend for volume concentrations, with a greater increase of particles in the size range of 0.5–1 μm during severe haze.

During the evolution from mild haze to severe haze, the number concentrations of particles larger than 50 nm and total surface concentrations increased by a factor of 1.65 and 1.52 respectively. The size shift of peaks of the number concentrations to larger particles was due to the aging of aerosol through condensation and coagulation, and the addition of ammonium, nitrate, primary and secondary organic species (Moffet et al., 2008; F. Yang et al., 2012).

### 3.3. Temporal characteristics of particle number concentration and size distribution in haze and photochemical smog

Three consecutive days were chosen for each of the haze, photochemical smog and clean days to understand the temporal patterns. The exact days were from April 6 to April 8, from May 9 to May 11 and from April 29 to May 1, as the representative of haze, photochemical smog and clean days, respectively. The weather conditions for these periods were visibility less than 10 km, RH lower than 80% and average wind speed 1.7 m/sec in haze days, visibility about 15 km, RH lower than 75% and average wind speed 3.6 m/sec in photochemical smog and visibility above 20 km, RH lower than 75% and average wind speed 6.7 m/sec in clean days.



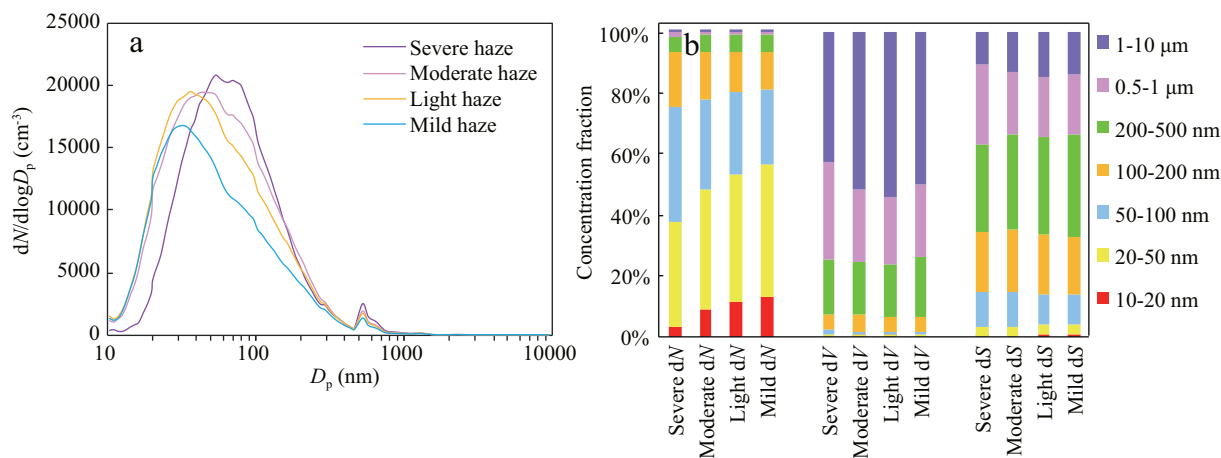


**Fig. 3 – Particle size distribution (a) and average percentages of particle number, volume and surface concentrations in different size ranges (b) under severe, moderate, light and mild haze. (Severe: severe haze; Moderate: moderate haze; Light: light haze; Mild: mild haze.)**

The diurnal variation of particle number concentrations in haze days had a binomial pattern, with two peaks at 8:00 a.m. and 10:00 p.m., as shown in Fig. 4. Increase of particle number concentrations in photochemical smog began at 6:00 a.m. and

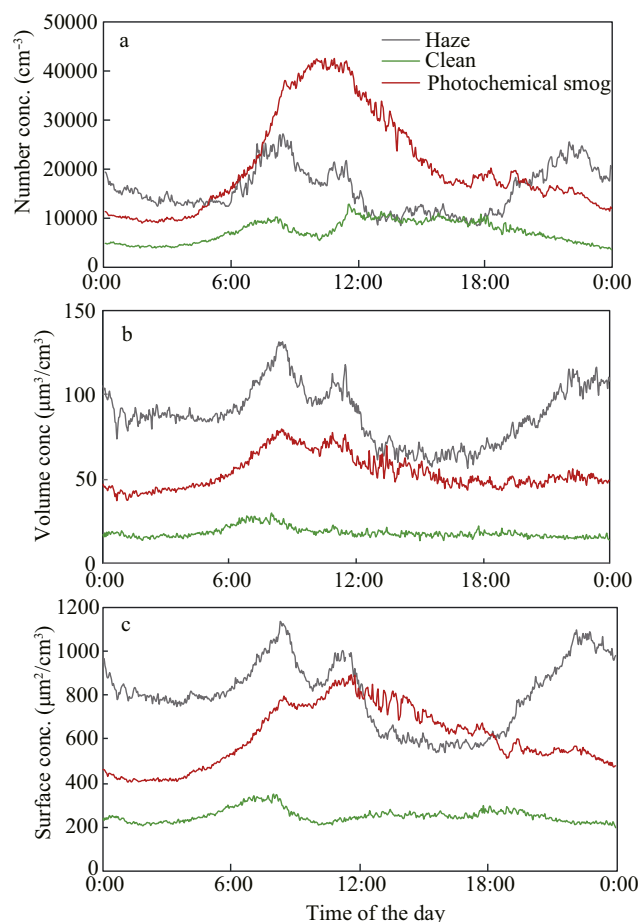


**Fig. 4 – Diurnal variations of particle number, volume and surface concentration in haze, photochemical smog and clean days.**

reached a peak at 11:00 a.m., corresponding to the morning rush hours, suggesting that particle concentrations increased rapidly as the photochemical reaction intensified, and showing the typical growth of particles.

As shown in Fig. 5, the temporal pattern of size distribution, there was a dramatic increase in large particles in the morning and the evening during haze days, a completely different pattern compared to photochemical smog episodes. There was not an apparent particle diminishing process in haze days.

In clean days, neither photochemical particle formation process nor particle accumulation process like those in haze days was observed. Ozone in clean days varied in the range of 40 to 80 ppb, generally smaller than the range of 20 to 145 ppb in photochemical smog episodes. The main reason for this was the dramatic decline in emissions, as the clean days were holidays, as well as the high wind speed, leading to faster dispersion.

Volume concentrations were higher all day during haze, reaching over 50 μm<sup>3</sup>/cm<sup>3</sup>. The diurnal pattern had a binomial distribution, peaking at a similar time as for the number concentration. The diurnal change of volume concentration was not obvious compared to the dramatic change of number concentration during photochemical smog. The change of surface concentration was similar to that of volume concentration. From noon to 6 p.m. only, the surface concentration in photochemical smog was larger than that in haze days. The great increase of particle number concentration from 50 to 100 nm was the greatest driver for the increase in surface concentration.

#### 3.4. Particle chemical composition in different size ranges during haze and photochemical smog

The sampling period of size-resolved particle chemical composition was from May 4 to June 2, and all selected samples were collected in the same time period as particle number concentration and size distribution for haze and photochemical smog episodes. The average of more than six samples is presented in Fig. 6.

The major ions in particles during haze and photochemical smog episodes were NH<sub>4</sub><sup>+</sup>, NO<sub>3</sub><sup>-</sup> and SO<sub>4</sub><sup>2-</sup>, contributing 73% and

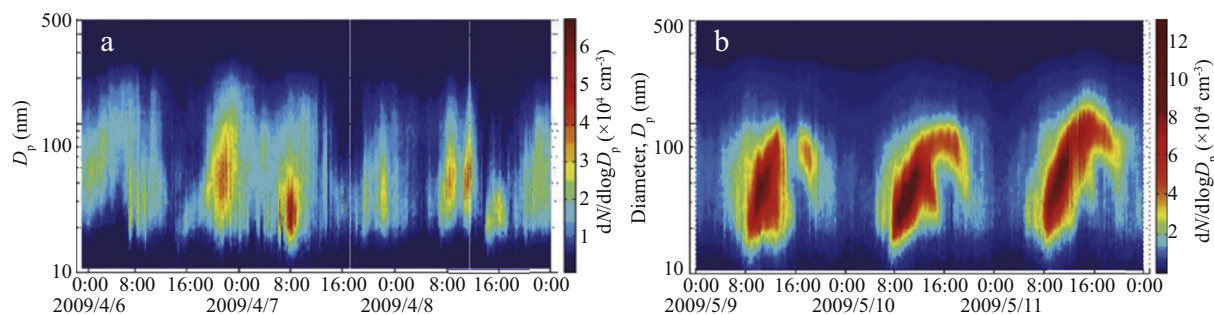


Fig. 5 – Temporal variations of particle size distributions in haze (a) and photochemical smog (b).

70% of the total soluble ions, respectively.  $\text{Na}^+$ ,  $\text{Cl}^-$  and  $\text{Ca}^{2+}$  contributed to 12% and 19% of the total soluble ions. Concentrations of all soluble ions increased during haze, of which  $\text{NH}_4^+$ ,  $\text{SO}_4^{2-}$  and  $\text{NO}_3^-$  increased greatly, and were 4.4, 3.6 and 3.2 times the values in photochemical smog episodes respectively. The next increase was followed by  $\text{Na}^+$ ,  $\text{K}^+$  and  $\text{Ca}^{2+}$ , 2.9, 2.6 and 2.1

times respectively. The increase of  $\text{Cl}^-$  concentration was relatively small by contrast.

Most  $\text{SO}_4^{2-}$  was observed in fine particles, peaking at the size range of 0.7–1.1  $\mu\text{m}$  in haze while at the size range of 0.4–0.7  $\mu\text{m}$  in photochemical smog. The size distribution of  $\text{NO}_3^-$  concentration in haze events extended from coarse particles to fine

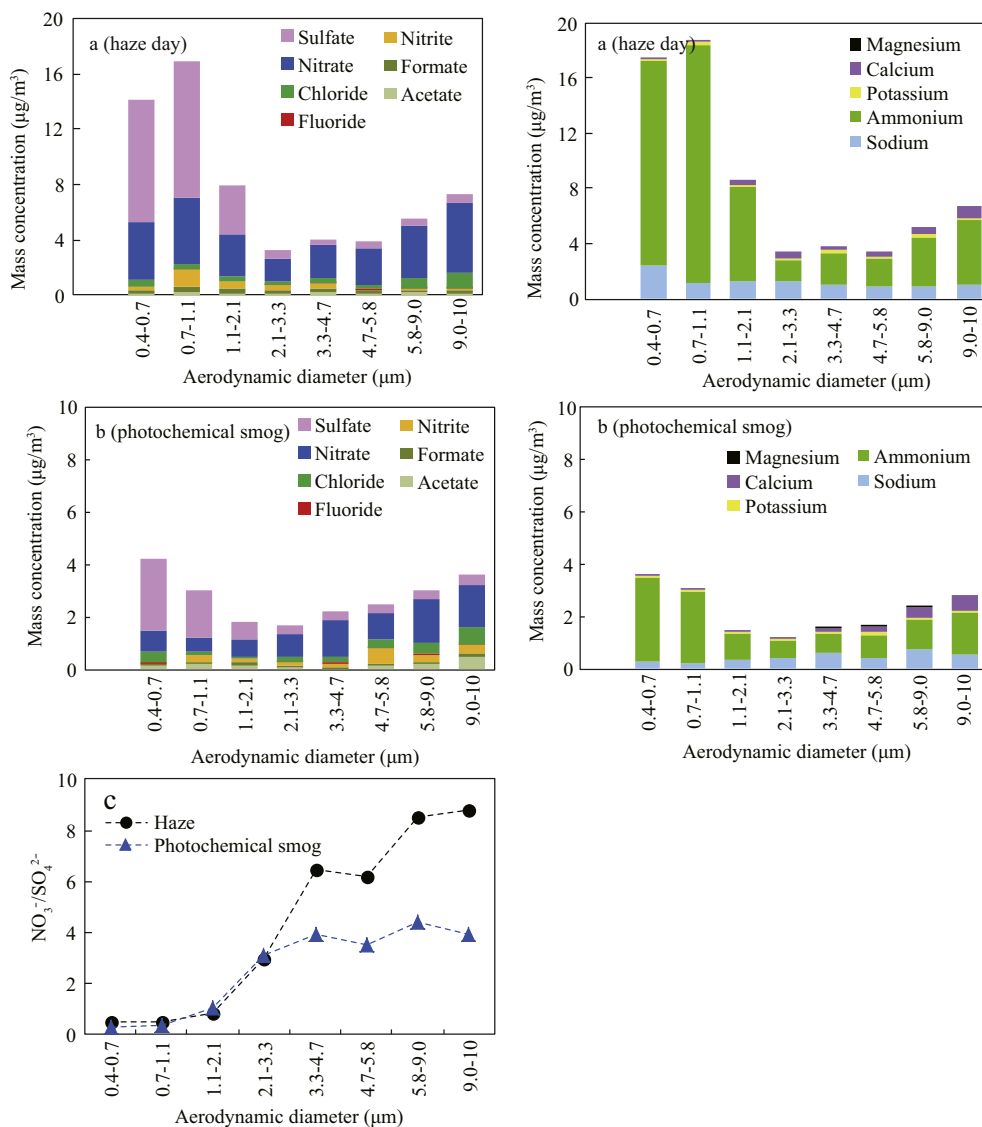


Fig. 6 – Particle chemical composition in different size ranges in haze (a) and photochemical smog (b), and  $\text{NO}_3^-/\text{SO}_4^{2-}$  (c).

particles, peaking at 0.4–0.7  $\mu\text{m}$  and 9.0–10  $\mu\text{m}$ ; but the  $\text{NO}_3^-$  concentration reached peaks in coarse particles during photochemical smog episodes. This was different from the results of Cheng et al. (2011) in Jinan, where the concentration of  $\text{NO}_3^-$  was high even in non-haze days. The concentration of  $\text{NH}_4^+$  peaked at the size ranges of 0.4–1.1  $\mu\text{m}$  and 5.8–10.0  $\mu\text{m}$ . Compared to coarse particles, the concentration of  $\text{NH}_4^+$  was much higher in fine particles smaller than 2.1  $\mu\text{m}$  during haze events. Combined with the dramatic increase of particle number concentration in haze events, we concluded that the increase of  $\text{SO}_4^{2-}$  and  $\text{NH}_4^+$  contributed most to the increase of particles in the range of 0.5–1  $\mu\text{m}$ . However, it was  $\text{NO}_3^-$  that played a vital role in the increase of total number concentration. The great increase of the three ions in fine particles suggests the important influence of secondary pollution.

$\text{Na}^+$  was mainly observed in coarse particles larger than 2.1  $\mu\text{m}$  during photochemical smog episodes, while it was increased in fine particles and peaked at 0.4–0.7  $\mu\text{m}$  during haze events. Compared to photochemical smog,  $\text{K}^+$  increased most and peaked in particles between 0.7 and 2.1  $\mu\text{m}$ , as it was in the fine particles resulting from biomass burning.  $\text{Cl}^-$  and  $\text{Ca}^{2+}$  increased most in coarse particles at 9–10  $\mu\text{m}$ , mainly from biomass burning and soil, respectively.

The average ratios of  $\text{NO}_3^-$  to  $\text{SO}_4^{2-}$  during haze and photochemical smog episodes were 1.12 and 1.26 respectively, suggesting that the major source of particles was mobile transportation during the sampling period. As shown in Fig. 6c, coarse particles larger than 3.3  $\mu\text{m}$  were dominated by nitrate while fine particles were dominated by sulfate. As the smallest particle size sampled in this study was 0.4  $\mu\text{m}$ , the actual  $\text{NO}_3^-/\text{SO}_4^{2-}$  ratio in  $\text{PM}_{10}$  should be estimated to be even smaller. The concentration ratios of  $\text{NO}_3^-$  and  $\text{SO}_4^{2-}$  in fine particles from 0.4 to 3.3  $\mu\text{m}$  in haze events were equivalent to those in photochemical smog episodes, but the ratios were reversed in coarse particles between 3.3 and 10  $\mu\text{m}$ .

## 4. Conclusions

Haze events were frequent in Shanghai, taking up 43% of the days in 2009. 30% of all the haze events were severe and moderate, and mainly occurred in winter and spring. 2.17% of the hourly ozone concentrations exceeded 100 ppbv all year, and more than half of the days of heavy ozone pollution were not haze days. The total particle number concentration of haze days was more than that of clean days, and less than that of photochemical smog days. The greatest increase of particle number concentration was in the size ranges of 0.5–1  $\mu\text{m}$  and 1–10  $\mu\text{m}$  during haze events, and was within the ranges of 50–100 nm and 100–200 nm during photochemical smog episodes. Particles larger than 200 nm, which only make up about 5% of the number concentration, composed 90% of the total volume concentration and particles larger than 1  $\mu\text{m}$  contributed 50%. During haze events, 90% of the surface concentration was from particles larger than 100 nm. The severity of haze was not directly associated with total particle number concentration, but was associated with the number concentration of larger particles, which was closely related to the size distribution of volume concentrations. Concentrations of all soluble ions were increased during haze events, of which  $\text{NH}_4^+$ ,  $\text{SO}_4^{2-}$  and  $\text{NO}_3^-$  increased most, followed by  $\text{Na}^+$ ,  $\text{K}^+$  and  $\text{Ca}^{2+}$ , then

$\text{Cl}^-$ . The size distribution of these ions was very different during haze and photochemical smog episodes. The average ratios of  $\text{NO}_3^-$  to  $\text{SO}_4^{2-}$  during haze and photochemical smog episodes were 1.12 and 1.26 respectively, suggesting that the major source of particles was mobile sources during the sampling period.

## Acknowledgments

This work was supported by the National Natural Science Foundation of China (Nos. 21190053, 21177025), the Shanghai Science and Technology Commission of Shanghai Municipality (Nos. 13XD1400700, 12DJ1400100), the Priority fields for Ph.D. Programs Foundation of the Ministry of Education of China (No. 20110071130003) and the Strategic Priority Research Program of the Chinese Academy of Sciences (No. XDB05010200).

## REFERENCES

- Andreae, M.O., Schmid, O., Yang, H., Chand, D., Yu, J.Z., Zeng, L.M., et al., 2008. Optical properties and chemical composition of the atmospheric aerosol in urban Guangzhou, China. *Atmos. Environ.* 42 (25), 6335–6350.
- Chen, X.L., Feng, Y.R., Li, J.N., Lin, W.S., Fan, S.J., Wang, A.Y., et al., 2009. Numerical simulations on the effect of sea-land breezes on atmospheric haze over the Pearl River Delta Region. *Environ. Model. Assess.* 14 (3), 351–363.
- Chen, J., Zhao, C.S., Ma, N., Liu, P.F., Gobel, T., Hallbauer, E., et al., 2012a. A parameterization of low visibilities for hazy days in the North China Plain. *Atmos. Chem. Phys.* 12 (11), 4935–4950.
- Chen, Y.H., Liu, Q., Geng, F.H., Zhang, H., Cai, C.J., Xu, T.T., et al., 2012b. Vertical distribution of optical and micro-physical properties of ambient aerosols during dry haze periods in Shanghai. *Atmos. Environ.* 50, 50–59.
- Cheng, S.H., Yang, L.X., Zhou, X.H., Xue, L.K., Gao, X.M., Zhou, Y., et al., 2011. Size-fractionated water-soluble ions, situ pH and water content in aerosol on hazy days and the influences on visibility impairment in Jinan, China. *Atmos. Environ.* 45 (27), 4631–4640.
- Du, H.H., Kong, L.D., Cheng, T.T., Chen, J.M., Du, J.F., Li, L., et al., 2011. Insights into summertime haze pollution events over Shanghai based on online water-soluble ionic composition of aerosols. *Atmos. Environ.* 45 (29), 5131–5137.
- Duan, J.C., Guo, S.J., Tan, J.H., Wang, S.L., Chai, F.H., 2012. Characteristics of atmospheric carbonyls during haze days in Beijing, China. *Atmos. Res.* 114, 17–27.
- Fu, Q.Y., Zhuang, G.S., Wang, J., Xu, C., Huang, K., Li, J., et al., 2008. Mechanism of formation of the heaviest pollution episode ever recorded in the Yangtze River Delta, China. *Atmos. Environ.* 42 (9), 2023–2036.
- Gao, J., Wang, T., Zhou, X.H., Wu, W.S., Wang, W.X., 2009. Measurement of aerosol number size distributions in the Yangtze River delta in China: formation and growth of particles under polluted conditions. *Atmos. Environ.* 43 (4), 829–836.
- Guo, S.J., Tan, J.H., Duan, J.C., Ma, Y.L., Yang, F.M., He, K.B., et al., 2012a. Characteristics of atmospheric non-methane hydrocarbons during haze episode in Beijing, China. *Environ. Monit. Assess.* 184 (12), 7235–7246.
- Guo, S.J., Yang, F.M., Tan, J.H., Duan, J.C., 2012b. Nonmethane hydrocarbons in ambient air of hazy and normal days in Foshan, South China. *Environ. Eng. Sci.* 29 (4), 262–269.
- Hou, B., Zhuang, G.S., Zhang, R., Liu, T.N., Guo, Z.G., et al., 2011. The implication of carbonaceous aerosol to the formation of

- haze: revealed from the characteristics and sources of OC/EC over a mega-city in China. *J. Hazard. Mater.* 190 (1–3), 529–536.
- Huang, K., Zhuang, G., Lin, Y., Fu, J.S., Wang, Q., Liu, T., et al., 2012. Typical types and formation mechanisms of haze in an Eastern Asia megacity, Shanghai. *Atmos. Chem. Phys.* 12 (1), 105–124.
- Li, S.S., Chen, L.F., Zheng, F.B., Han, D., Wang, Z.F., 2009. Design and application of haze optic Thickness Retrieval model for Beijing Olympic Games. *Proceedings of the IEEE International Geoscience and Remote Sensing Symposium*, Cape Town, Jul 12–17.
- Li, W.J., Shao, L.Y., Buseck, P.R., 2010. Haze types in Beijing and the influence of agricultural biomass burning. *Atmos. Chem. Phys.* 10 (17), 8119–8130.
- Li, W.J., Zhou, S.Z., Wang, X.F., Xu, Z., Yuan, C., Yu, Y.C., et al., 2011. Integrated evaluation of aerosols from regional brown hazes over northern China in winter: concentrations, sources, transformation, and mixing states. *J. Geophys. Res.* 116, D9. <http://dx.doi.org/10.1029/2010JD015099>.
- Lu, H.X., Cai, Q.Y., Wen, S., Chi, Y.G., Guo, S.J., Sheng, G.Y., et al., 2009. Carbonyl compounds in the ambient air of hazy days and clear days in Guangzhou, China. *Atmos. Res.* 94 (3), 363–372.
- Ma, J.Z., Chen, Y., Wang, W., Yan, P., Liu, H.J., Yang, S.Y., et al., 2010. Strong air pollution causes widespread haze-clouds over China. *J. Geophys. Res.* 115, D18. <http://dx.doi.org/10.1029/2009JD013065>.
- Ma, J.Z., Xu, X.B., Zhao, C.S., Yan, P., 2012. A review of atmospheric chemistry research in China: photochemical smog, haze pollution, and gas-aerosol interactions. *Adv. Atmos. Sci.* 29 (5), 1006–1025.
- Moffet, R.C., de Foy, B., Molina, L.T., Molina, M.J., Prather, K.A., 2008. Measurement of ambient aerosols in northern Mexico City by single particle mass spectrometry. *Atmos. Chem. Phys.* 8, 4499–4516.
- Quan, J., Zhang, Q., He, H., Liu, J., Huang, M., Jin, H., 2011. Analysis of the formation of fog and haze in North China Plain (NCP). *Atmos. Chem. Phys.* 11 (15), 8205–8214.
- Shi, Z.B., He, K.B., Yu, X.C., Yao, Z.L., Yang, F.M., Ma, Y.L., et al., 2007. Diurnal variation of number concentration and size distribution of ultrafine particles in the urban atmosphere of Beijing in winter. *J. Environ. Sci.* 19 (8), 933–938.
- Sun, Y.L., Zhuang, G.S., Tang, A.H., Wang, Y., An, Z.S., 2006. Chemical characteristics of PM<sub>2.5</sub> and PM<sub>10</sub> in haze-fog episodes in Beijing. *Environ. Sci. Technol.* 40 (10), 3148–3155.
- Tan, J.H., Duan, J.C., He, K.B., Ma, Y.L., Duan, F.K., Chen, Y., et al., 2009. Chemical characteristics of PM<sub>2.5</sub> during a typical haze episode in Guangzhou. *J. Environ. Sci.* 21 (6), 774–781.
- Tan, J.H., Guo, S.J., Ma, Y.L., Duan, J.C., Cheng, Y., He, K.B., et al., 2011. Characteristics of particulate PAHs during a typical haze episode in Guangzhou, China. *Atmos. Res.* 102 (1–2), 91–98.
- Tao, M.H., Chen, L.F., Su, L., Tao, J.H., 2012. Satellite observation of regional haze pollution over the North China Plain. *J. Geophys. Res.* 117. <http://dx.doi.org/10.1029/2012JD017915>.
- Wang, Y., Zhuang, G.S., Sun, Y.L., An, Z.S., 2006. The variation of characteristics and formation mechanisms of aerosols in dust, haze, and clear days in Beijing. *Atmos. Environ.* 40 (34), 6579–6591.
- Wang, X.M., Ding, X., Fu, X.X., He, Q.F., Wang, S.Y., Bernard, F., et al., 2012a. Aerosol scattering coefficients and major chemical compositions of fine particles observed at a rural site hit the central Pearl River Delta, South China. *J. Environ. Sci.* 24 (1), 72–77.
- Wang, Z.T., Li, Q., Li, S.S., Chen, L.F., Zhou, C.Y., Wang, Z.F., et al., 2012b. The monitoring of haze from HJ-1. *Spectrosc. Spectr. Anal.* 32 (3), 775–780.
- Wu, D., Bi, X.Y., Deng, X.J., Li, F., Tan, H.B., Liao, G.L., et al., 2007. Effect of atmospheric haze on the deterioration of visibility over the Pearl River Delta. *Acta Meteorol. Sin.* 21 (2), 215–223.
- Xiao, Z.M., Zhang, Y.F., Hong, S.M., Bi, X.H., Jiao, L., Feng, Y.C., et al., 2011. Estimation of the main factors influencing haze, based on a long-term monitoring campaign in Hangzhou, China. *Aerosol Air Qual. Res.* 11 (7), 873–882.
- Xu, H.J., Wang, X.M., Pösch, U., Feng, S.L., Wu, D., Yang, L., et al., 2008. Genotoxicity of total and fractionated extractable organic matter in fine air particulate matter from urban Guangzhou: comparison between haze and nonhaze episodes. *Environ. Toxicol. Chem.* 27 (1), 206–212.
- Yang, F., Chen, H., Du, J.F., Yang, X., Gao, S., Chen, J.M., et al., 2012a. Evolution of the mixing state of fine aerosols during haze events in Shanghai. *Atmos. Res.* 104, 193–201.
- Yang, T., Wang, X.Q., Wang, Z.F., Sun, Y.L., Zhang, W., Zhang, B., et al., 2012b. Gravity-current driven transport of haze from North China Plain to Northeast China in winter 2010 — part I: observations. *Sola* 8, 13–16.
- Ye, X.N., Ma, Z., Zhang, J.C., Du, H.H., Chen, J.M., Chen, H., et al., 2011. Important role of ammonia on haze formation in Shanghai. *Environ. Res. Lett.* 6 (2). <http://dx.doi.org/10.1088/1748-9326/6/2/024019>.
- Yu, X.N., Zhu, B., Yin, Y., Yang, J., Li, Y.W., Bu, X.L., 2011. A comparative analysis of aerosol properties in dust and haze-fog days in a Chinese urban region. *Atmos. Res.* 99 (2), 241–247.
- Yuan, Y., Liu, S.S., Castro, R., Pan, X.B., 2012. PM<sub>2.5</sub> monitoring and mitigation in the cities of China. *Environ. Sci. Technol.* 46 (7), 3627–3628.
- Zhang, Y.H., Huang, W., London, S.J., Song, G.X., Chen, G.H., Jiang, L.L., et al., 2006. Ozone and daily mortality in Shanghai, China. *Environ. Health Perspect.* 114 (8), 1227–1232.
- Zhang, A.D., Wang, X.Y., Xiu, G.L., 2007. Pollution characteristics and variation patterns of ozone in low-level air in central urban area of Shanghai. *Shanghai Environ. Sci.* 26 (2), 62–76.
- Zhang, M., Wang, X.M., Chen, J.M., Cheng, T.T., Wang, T., Yang, X., et al., 2010. Physical characterization of aerosol particles during the Chinese New Year's firework events. *Atmos. Environ.* 44 (39), 5191–5198.





## Editorial Board of Journal of Environmental Sciences

### Editor-in-Chief

**Hongxiao Tang** Research Center for Eco-Environmental Sciences, Chinese Academy of Sciences, China

### Associate Editors-in-Chief

**Jiuhui Qu** Research Center for Eco-Environmental Sciences, Chinese Academy of Sciences, China  
**Shu Tao** Peking University, China  
**Nigel Bell** Imperial College London, United Kingdom  
**Po-Keung Wong** The Chinese University of Hong Kong, Hong Kong, China

### Editorial Board

#### Aquatic environment

**Baoyu Gao**  
Shandong University, China  
**Maohong Fan**  
University of Wyoming, USA  
**Chihpin Huang**  
National Chiao Tung University  
Taiwan, China  
**Ng Wun Jern**  
Nanyang Environment &  
Water Research Institute, Singapore  
**Clark C. K. Liu**  
University of Hawaii at Manoa, USA  
**Hokyoung Shon**  
University of Technology, Sydney, Australia  
**Zijian Wang**  
Research Center for Eco-Environmental Sciences,  
Chinese Academy of Sciences, China  
**Zhiwu Wang**  
The Ohio State University, USA  
**Yuxiang Wang**  
Queen's University, Canada  
**Min Yang**  
Research Center for Eco-Environmental Sciences,  
Chinese Academy of Sciences, China  
**Zhifeng Yang**  
Beijing Normal University, China  
**Han-Qing Yu**  
University of Science & Technology of China  
**Terrestrial environment**  
**Christopher Anderson**  
Massey University, New Zealand  
**Zucong Cai**  
Nanjing Normal University, China  
**Xinbin Feng**  
Institute of Geochemistry,  
Chinese Academy of Sciences, China  
**Hongqing Hu**  
Huazhong Agricultural University, China  
**Kin-Che Lam**  
The Chinese University of Hong Kong  
Hong Kong, China  
**Erwin Klumpp**  
Research Centre Juelich, Agrosphere Institute  
Germany  
**Peijun Li**  
Institute of Applied Ecology,  
Chinese Academy of Sciences, China

#### Michael Schloter

German Research Center for Environmental Health  
Germany  
**Xuejun Wang**  
Peking University, China  
**Lizhong Zhu**  
Zhejiang University, China  
**Atmospheric environment**  
**Jianmin Chen**  
Fudan University, China  
**Abdelwahid Mellouki**  
Centre National de la Recherche Scientifique  
France  
**Yujing Mu**  
Research Center for Eco-Environmental Sciences,  
Chinese Academy of Sciences, China  
**Min Shao**  
Peking University, China  
**James Jay Schauer**  
University of Wisconsin-Madison, USA  
**Yuesi Wang**  
Institute of Atmospheric Physics,  
Chinese Academy of Sciences, China  
**Xin Yang**  
University of Cambridge, UK  
**Environmental biology**  
**Yong Cai**  
Florida International University, USA  
**Henner Hollert**  
RWTH Aachen University, Germany  
**Jae-Seong Lee**  
Sungkyunkwan University, South Korea  
**Christopher Rensing**  
University of Copenhagen, Denmark  
**Bojan Sedmak**  
National Institute of Biology, Slovenia  
**Lirong Song**  
Institute of Hydrobiology,  
Chinese Academy of Sciences, China  
**Chunxia Wang**  
National Natural Science Foundation of China  
**Gehong Wei**  
Northwest A & F University, China  
**Daqiang Yin**  
Tongji University, China  
**Zhongtang Yu**  
The Ohio State University, USA

#### Environmental toxicology and health

**Jingwen Chen**  
Dalian University of Technology, China  
**Jianying Hu**  
Peking University, China  
**Guibin Jiang**  
Research Center for Eco-Environmental Sciences,  
Chinese Academy of Sciences, China  
**Sijin Liu**  
Research Center for Eco-Environmental Sciences,  
Chinese Academy of Sciences, China  
**Tsuyoshi Nakanishi**  
Gifu Pharmaceutical University, Japan  
**Willie Peijnenburg**  
University of Leiden, The Netherlands  
**Bingsheng Zhou**  
Institute of Hydrobiology,  
Chinese Academy of Sciences, China  
**Environmental catalysis and materials**  
**Hong He**  
Research Center for Eco-Environmental Sciences,  
Chinese Academy of Sciences, China  
**Junhua Li**  
Tsinghua University, China  
**Wenfeng Shangguan**  
Shanghai Jiao Tong University, China  
**Yasutake Teraoka**  
Kyushu University, Japan  
**Ralph T. Yang**  
University of Michigan, USA  
**Environmental analysis and method**  
**Zongwei Cai**  
Hong Kong Baptist University,  
Hong Kong, China  
**Jiping Chen**  
Dalian Institute of Chemical Physics,  
Chinese Academy of Sciences, China  
**Minghui Zheng**  
Research Center for Eco-Environmental Sciences,  
Chinese Academy of Sciences, China  
**Municipal solid waste and green chemistry**  
**Pinjing He**  
Tongji University, China  
**Environmental ecology**  
**Rusong Wang**  
Research Center for Eco-Environmental Sciences,  
Chinese Academy of Sciences, China

### Editorial office staff

**Managing editor** Qingcai Feng  
**Editors** Zixuan Wang Suqin Liu Zhengang Mao  
**English editor** Catherine Rice (USA)

# JOURNAL OF ENVIRONMENTAL SCIENCES

环境科学学报(英文版)  
(<http://www.jesc.ac.cn>)

## Aims and scope

*Journal of Environmental Sciences* is an international academic journal supervised by Research Center for Eco-Environmental Sciences, Chinese Academy of Sciences. The journal publishes original, peer-reviewed innovative research and valuable findings in environmental sciences. The types of articles published are research article, critical review, rapid communications, and special issues.

The scope of the journal embraces the treatment processes for natural groundwater, municipal, agricultural and industrial water and wastewaters; physical and chemical methods for limitation of pollutants emission into the atmospheric environment; chemical and biological and phytoremediation of contaminated soil; fate and transport of pollutants in environments; toxicological effects of terrorist chemical release on the natural environment and human health; development of environmental catalysts and materials.

## For subscription to electronic edition

Elsevier is responsible for subscription of the journal. Please subscribe to the journal via <http://www.elsevier.com/locate/jes>.

## For subscription to print edition

China: Please contact the customer service, Science Press, 16 Donghuangchenggen North Street, Beijing 100717, China. Tel: +86-10-64017032; E-mail: [journal@mail.sciencep.com](mailto:journal@mail.sciencep.com), or the local post office throughout China (domestic postcode: 2-580).

Outside China: Please order the journal from the Elsevier Customer Service Department at the Regional Sales Office nearest you.

## Submission declaration

Submission of an article implies that the work described has not been published previously (except in the form of an abstract or as part of a published lecture or academic thesis), that it is not under consideration for publication elsewhere. The submission should be approved by all authors and tacitly or explicitly by the responsible authorities where the work was carried out. If the manuscript accepted, it will not be published elsewhere in the same form, in English or in any other language, including electronically without the written consent of the copyright-holder.

## Submission declaration

Submission of the work described has not been published previously (except in the form of an abstract or as part of a published lecture or academic thesis), that it is not under consideration for publication elsewhere. The publication should be approved by all authors and tacitly or explicitly by the responsible authorities where the work was carried out. If the manuscript accepted, it will not be published elsewhere in the same form, in English or in any other language, including electronically without the written consent of the copyright-holder.

## Editorial

Authors should submit manuscript online at <http://www.jesc.ac.cn>. In case of queries, please contact editorial office, Tel: +86-10-62920553, E-mail: [jesc@263.net](mailto:jesc@263.net), [jesc@rcees.ac.cn](mailto:jesc@rcees.ac.cn). Instruction to authors is available at <http://www.jesc.ac.cn>.

## Journal of Environmental Sciences (Established in 1989)

Vol. 26 No. 9 2014

<b>Supervised by</b>	Chinese Academy of Sciences	<b>Published by</b>	Science Press, Beijing, China
<b>Sponsored by</b>	Research Center for Eco-Environmental Sciences, Chinese Academy of Sciences		Elsevier Limited, The Netherlands
<b>Edited by</b>	Editorial Office of Journal of Environmental Sciences P. O. Box 2871, Beijing 100085, China Tel: 86-10-62920553; <a href="http://www.jesc.ac.cn">http://www.jesc.ac.cn</a> E-mail: <a href="mailto:jesc@263.net">jesc@263.net</a> , <a href="mailto:jesc@rcees.ac.cn">jesc@rcees.ac.cn</a>	<b>Distributed by</b>	Domestic Science Press, 16 Donghuangchenggen North Street, Beijing 100717, China Local Post Offices through China Foreign Elsevier Limited <a href="http://www.elsevier.com/locate/jes">http://www.elsevier.com/locate/jes</a>
<b>Editor-in-chief</b>	Hongxiao Tang	<b>Printed by</b>	Beijing Beilin Printing House, 100083, China
CN 11-2629/X	Domestic postcode: 2-580		Domestic price per issue RMB ¥ 110.00

ISSN 1001-0742

